

## Random telegraph signal and $1/f$ noise in forward-biased single-walled carbon nanotube film-silicon Schottky junctions

Yanbin An, Hemant Rao, Gijs Bosman, and Ant Ural<sup>a)</sup>

*Department of Electrical and Computer Engineering, University of Florida, Gainesville, Florida 32611, USA*

(Received 8 March 2012; accepted 1 May 2012; published online 21 May 2012)

The electronic noise of single-walled carbon nanotube (CNT) film-Silicon Schottky junctions under forward bias is experimentally characterized. The superposition of a stable  $1/f$  noise and a temporally unstable Lorentzian noise is observed, along with a random telegraph signal (RTS) in the time domain. The data analysis shows that the Lorentzian noise results from the RTS current fluctuations. The data agree well with theoretical descriptions of noise in Schottky junctions due to carrier trapping and detrapping at interface states. Understanding the noise properties of CNT film-Si junctions is important for the integration of CNT film electrodes into silicon-based devices.

© 2012 American Institute of Physics. [<http://dx.doi.org/10.1063/1.4719094>]

Single-walled carbon nanotube (CNT) films have recently attracted significant research attention for optoelectronic and photovoltaic device applications, such as solar cells, light-emitting diodes (LEDs), and photodetectors,<sup>1–5</sup> in which they can be used as transparent, conductive, and flexible electrodes.<sup>6</sup> An application of great importance is the integration of CNT film electrodes into conventional semiconductor devices, in particular those based on silicon, since it is the most widely used semiconductor material. We have recently shown that CNT films form a Schottky junction on Si with a zero-bias barrier height of 0.435 eV for  $p$ -type Si.<sup>7</sup> Several recent studies have demonstrated solar cells and photodetectors based on such CNT film-Si Schottky junctions.<sup>3,4,8–10</sup> The ultimate sensitivity of any electronic device is limited by fluctuations. Particularly for sensors and photodetectors, electrical noise is an important property that in most cases limits the device performance. There have been a number of recent studies on the noise properties of individual CNTs, CNT networks, and CNT films.<sup>11–14</sup> However, the noise properties of junction devices involving CNT films, and in particular CNT film-Si junctions, have not been studied previously.

In this Letter, we experimentally characterize the noise properties of CNT film/ $p$ -type silicon metal-semiconductor (MS) Schottky junctions under forward bias, where the CNT film acts as the metal and Si as the semiconductor. We observe a strong Lorentzian noise component in addition to  $1/f$  noise, and a random telegraph signal (RTS) in the time domain. We analyze the properties of both the  $1/f$  and Lorentzian noise and extract important parameters, such as the current dependence of the  $1/f$  noise and the characteristic frequency of the Lorentzian. Furthermore, the analysis of the time-domain data based on the theory of a two-level asymmetric RTS confirms that the Lorentzian noise in the frequency domain results from the RTS fluctuations in the time domain. We also find that while the  $1/f$  noise is stable, the RTS noise is temporally unstable. The data agree well with theoretical descriptions of noise in Schottky junctions due to carrier trapping and detrapping at interface states. These

results suggest that advances in the CNT film fabrication and deposition processes that minimize interface defects would significantly improve the noise properties of CNT film-Si junctions, which is important for optoelectronic, photovoltaic, and sensor devices incorporating CNT film electrodes on silicon.

The CNT film-Si MS junctions were fabricated as explained in detail previously.<sup>7</sup> Briefly, the device fabrication process started with a  $\sim 10^{16} \text{ cm}^{-3}$  doped  $p$ -type Si substrate having a  $\sim 400 \text{ nm}$  thermally grown  $\text{SiO}_2$  layer on top. After windows were opened in the  $\text{SiO}_2$  layer to define the MS contact areas, a CNT film of  $\sim 50 \text{ nm}$  nominal thickness prepared by vacuum filtration was deposited on the substrate and subsequently patterned by photolithography and  $\text{O}_2$  plasma etching. This was followed by Cr/Pd (10/90 nm) metal contact ring deposition by e-beam evaporation and lift-off. Figure 1(a) shows a 3D schematic of the completed device. More detailed fabrication and characterization results can be found in Refs. 3, 7, and 15.

The DC characterization of the CNT film-Si junctions was performed using an HP 4155B semiconductor parameter analyzer. Figure 1(b) shows the  $I$ - $V$  characteristics of the CNT film/ $p$ -type Si MS junction, depicting strong rectification consistent with our previous work in which a zero-bias Schottky barrier height of 0.435 eV was extracted from temperature dependent  $I$ - $V$  measurements.<sup>7</sup> The measurement of the low frequency current noise spectral density  $S_I$  at various forward biases was performed using a battery-powered low noise current preamplifier (SR 570). A spectrum analyzer (HP 3561A) was employed to analyze the noise spectra, and the time domain RTS noise was measured simultaneously using a digital data acquisition system (Agilent U2542A) operating at a sampling rate of 200 kHz.

Figure 2(a) shows  $S_I$  measured from 1 to 5 kHz at a forward bias of 1.04, 1.97, and 2.41 V. Due to the high resistivity of the CNT film-Si junction and the cut-off frequency of the current preamplifier, no  $S_I$  data beyond 5 kHz could be measured. As seen in Fig. 2(a), the noise spectra depict deviations from a pure  $1/f$ -type behavior and can be expressed as the superposition of a  $1/f$  noise component  $S_I^{1/f}$  and a Lorentzian noise component  $S_I^L$  as

<sup>a)</sup> Author to whom correspondence should be addressed. Electronic mail: antural@ufl.edu.

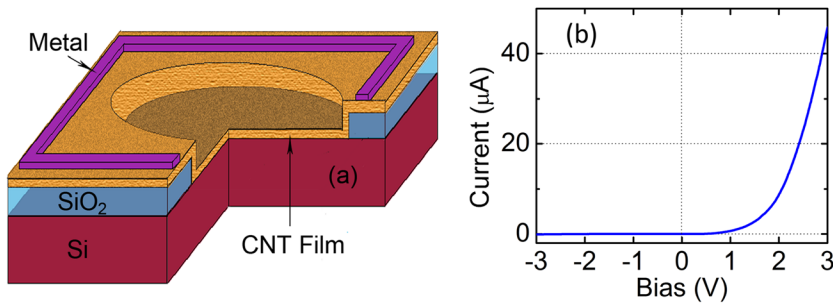


FIG. 1. (a) The 3D schematic of the fabricated CNT film-Si MS device showing both the top and cross-sectional views. (b) I-V characteristics of the CNT film/*p*-type Si MS device in the voltage bias range from  $-3$  V to  $3$  V at room temperature. Note that the polarity of the voltage bias is defined such that positive values correspond to forward bias.

$$S_I(f) = S_I^{1/f} + S_I^L = \frac{A \cdot I^\beta}{f^\gamma} + \frac{S_0}{1 + (f/f_c)^2}, \quad (1)$$

where  $A$  is the relative amplitude of the  $1/f$  noise,  $I$  is the DC current,  $f$  is the frequency,  $\beta$  and  $\gamma$  are constant exponents ( $\gamma \approx 1$  for  $1/f$  noise), and  $S_0$  is the plateau value and  $f_c$  is the characteristic frequency of the Lorentzian noise component.<sup>16,17</sup>

We first analyze the  $1/f$  noise component. The noise spectrum from Fig. 2(a) at  $1.97$  V forward bias is replotted in Fig. 2(b). The value of  $f_c$  in Eq. (1) can be determined from the maximum of the plot of  $S_I \times f$  vs.  $f$ , and the Lorentzian fitting can be done based on this extraction, as shown by the short dashed line in Fig. 2(b). The fitting result yields  $f_c = 40$  Hz and  $S_0 = 2.1 \times 10^{-17}$  A<sup>2</sup>/Hz. The  $1/f$  noise component can be obtained by subtracting the Lorentzian component from the total measured  $S_I$ , as indicated in Fig. 2(b). Fig. 2(b) also shows a power law fit to the extracted  $1/f$  noise component yielding an exponent  $\gamma = 1.1$ , confirming that the background noise is  $1/f$  type. By averaging the extracted  $1/f$  noise-component spectral densities from three separate measurements,  $S_I^{1/f}$  as a function of DC current  $I$  at a frequency of  $10$  Hz is plotted in the inset of Fig. 2(b). The data can be fit by a power law dependence  $S_I^{1/f} \propto I^\beta$  as shown by the dashed line in the inset with an exponent  $\beta = 0.92$ . This value of  $\beta$  agrees well with the theoretical model of  $1/f$  noise in forward biased Schottky barrier diodes operating in the thermionic-emission mode, which predicts  $S_I^{1/f} \propto I$ .<sup>16</sup> Our previous work has demonstrated that the dominant current transport mechanism in CNT film-Si junctions at room temperature is thermionic emission,<sup>7</sup> which is in agreement with the observed dependence of  $1/f$  noise on the DC current.

To further investigate the Lorentzian noise component, time-domain current fluctuations were recorded simultaneously, which exhibited up and down fluctuations characteristic of two-level asymmetric RTS noise. The inset of Fig. 2(a) shows the typical RTS fluctuations observed during a time period of  $500$  ms at a forward bias of  $1.04$  V. In this measurement, the RTS amplitude  $\Delta I$  is  $28.2$  nA, indicating a  $0.4\%$  relative current fluctuation. Since previous studies reveal that the CNT film itself does not exhibit RTS noise,<sup>14</sup> the origin of the observed RTS noise is most likely interface traps at the CNT film-Si junction causing fluctuations in the Schottky barrier height.<sup>16–19</sup> The solution-based CNT film deposition process in ambient conditions makes the interface between the CNT film and Si more prone to defects and interface traps compared to conventional metal-Si Schottky junctions. Furthermore, the CNT film consists of an interwoven percolating network of many nanotubes, making a non-

uniform, nonplanar, and spatially inhomogeneous contact with the Si substrate.<sup>7</sup> The barrier height between the Si substrate and metallic/semiconducting nanotubes in the CNT film with various chirality, diameter, and doping levels is expected to exhibit a statistical distribution. The barrier

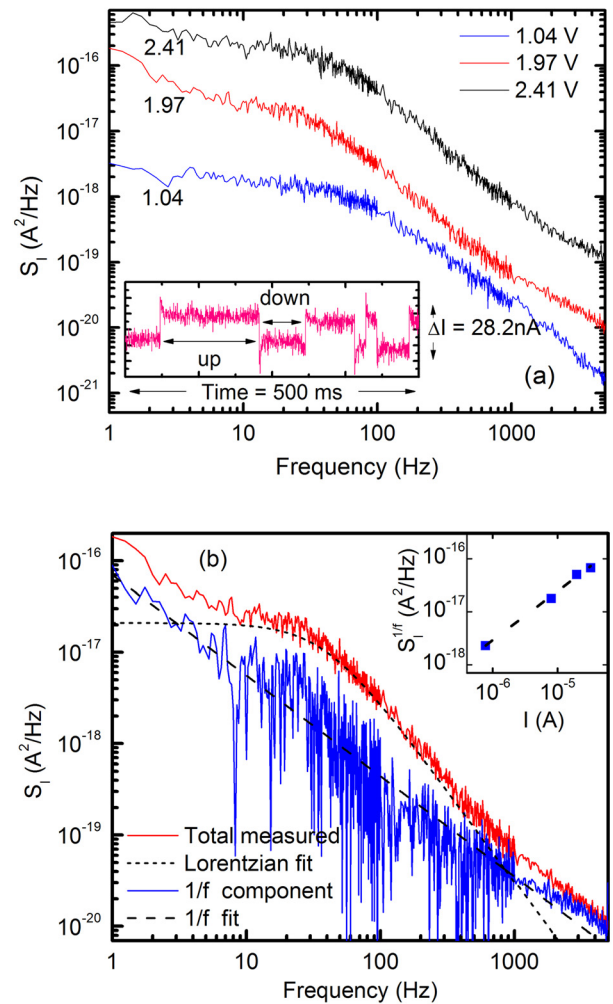


FIG. 2. (a) Low frequency current noise spectral density of the CNT film-Si MS junction measured at three different forward biases ( $1.04$ ,  $1.97$ , and  $2.41$  V as labeled), showing a strong Lorentzian noise component on top of a  $1/f$  noise component. The inset shows the time-domain current fluctuations at  $1.04$  V in a time frame of  $500$  ms, characteristic of a two-level asymmetric RTS noise. (b) The total measured current noise spectral density at  $1.97$  V from part (a) (red line), the Lorentzian component obtained from fitting the data (short dashed line), and the  $1/f$  noise component obtained by subtracting the Lorentzian component from the total measured  $S_I$  (blue line). The dashed line is a power law fit to the extracted  $1/f$  noise component yielding an exponent of  $\gamma = 1.1$ . The inset shows  $S_I^{1/f}$  averaged over three measurements as a function of forward bias current  $I$  at a frequency of  $10$  Hz.

height extracted in previous studies represents an “effective” value resulting from ensemble averaging.<sup>7</sup> As a result, if a defect is located at a bottleneck for current flow at the CNT film-Si interface, the trapping and detrapping of carriers there will have a strong impact on the current and produce RTS noise. Another possible origin of the RTS noise could be the presence of a thin native oxide layer at the CNT film-Si interface, which forms due to the porous nature of the CNT film, as discussed in previous studies.<sup>3,7</sup> Carrier trapping and detrapping at the Si-oxide interface is also a widely observed source for RTS noise.<sup>18,20</sup>

Noise measurements were also carried out on different days. Although the  $1/f$  noise component was stable and repeatable, the Lorentzian noise component and the RTS fluctuations were found to be temporally unstable. However, within a time frame of several hours to a day, the Lorentzian noise spectra and the RTS fluctuations were stable, enabling reliable measurements to be taken. Figure 3(a) shows measurements taken on three different days (labeled Measurements 1, 2, and 3) at an identical forward bias of 1.97 V, which depict changes in both the location of  $f_c$  and the value of  $S_0$ . Extracting the  $1/f$  noise component of the three meas-

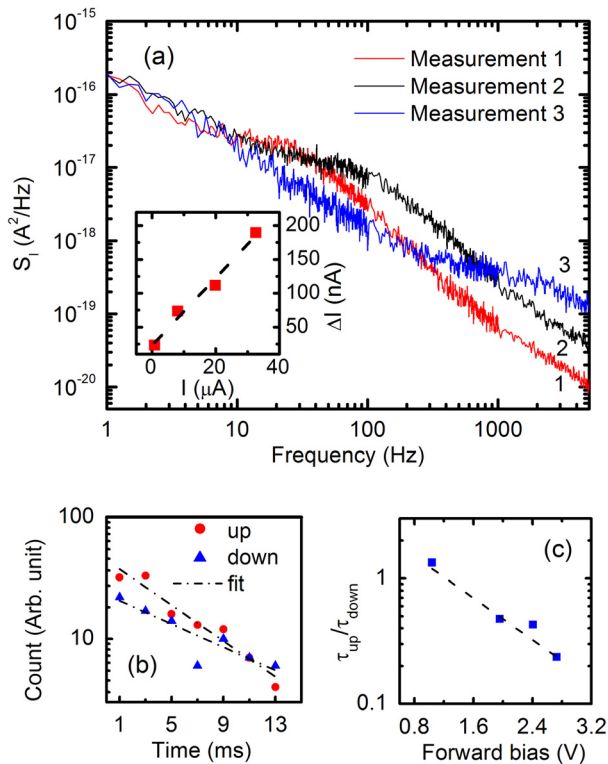


FIG. 3. (a) Low frequency current noise spectral density of the CNT film-Si MS device at 1.97 V forward bias measured on three different days (labeled as measurements 1, 2, and 3). Note that Measurement 1 is the same as the 1.97 V curve in Fig. 2(a). The change in both the location of  $f_c$  and the value of  $S_0$  is evident, indicating temporally unstable RTS noise. The inset shows the RTS amplitude  $\Delta I$  as a function of the forward current  $I$ . (b) Statistical distribution of the time durations of the up and down states for Measurement 1 recorded simultaneously as the noise spectra shown in part (a). The exponential fitting to Poisson distributions as shown in the figure gives an average lifetime of  $\tau_{up} = 5.81$  ms and  $\tau_{down} = 8.55$  ms. (c) A semi-log plot of  $\tau_{up}/\tau_{down}$  as a function of forward bias voltage for Measurement 1. The extrapolation of the exponential best fit as shown by the dashed line gives the zero-bias trap level with respect to the Fermi level as  $E_T = 32.7$  meV.

urements as done in Fig. 2(b), we find that the  $1/f$  noise component is almost identical in all three cases. The origin of the unstable RTS noise could be due to the presence of metastable interface defects or due to the migration of interface defects at the CNT film-Si junction.<sup>18,19</sup>

We next analyze the time-domain RTS noise data based on the theory of a two-level asymmetric random telegraph signal<sup>21</sup> and compare it with the parameters extracted from the frequency domain. A simple two-level RTS can be defined by three parameters: average lifetime of the up (high current) state  $\tau_{up}$ , average lifetime of the down (low current) state  $\tau_{down}$ , and the RTS amplitude  $\Delta I$ . The individual time durations of the up and down states are expected to statistically follow a Poisson distribution given by  $p_{up,down}(t) = (1/\tau_{up,down})\exp(-t/\tau_{up,down})$ , where  $p_{up}(t)$  is the probability per unit time that after time  $t$  the up-state has not made a transition, and then at time  $t$  switches to the down-state.<sup>18,21</sup> The reverse holds for  $p_{down}(t)$ . The statistical results from the time-domain data simultaneously recorded with the noise spectrum of Measurement 1 in Fig. 3(a) are plotted in Fig. 3(b). The exponential fitting to a Poisson distribution shown in the figure gives an average lifetime of  $\tau_{up} = 5.81$  ms and  $\tau_{down} = 8.55$  ms.

The current noise spectral density of a two-level RTS can be found by taking the Fourier transform of the autocorrelation of the signal as<sup>21</sup>

$$S_I(f) = \left[ \frac{4(\Delta I)^2 \tau_{eff}^2}{\tau_{up} + \tau_{down}} \right] \frac{1}{1 + 4\pi^2 f^2 \tau_{eff}^2}, \quad (2)$$

where  $\tau_{eff}$  is defined by  $1/\tau_{eff} = 1/\tau_{up} + 1/\tau_{down}$ . Comparing the  $S_I^L$  term in Eqs. (1) and (2), we see that the RTS results in a Lorentzian spectrum with  $f_c = 1/2\pi\tau_{eff}$  and  $S_0 = 4(\Delta I)^2 \tau_{eff}^2 / (\tau_{up} + \tau_{down})$ . Using these equations, we get  $f_c = 46$  Hz and  $S_0 = 1.9 \times 10^{-17}$  A<sup>2</sup>/Hz from the time domain analysis, which is in good agreement with the frequency domain fitting results given earlier and shown in Fig. 2(b). The values of  $\tau_{up}$ ,  $\tau_{down}$ ,  $f_c$ , and  $S_0$  obtained from the time domain analysis, as well as the values of  $f_c$  and  $S_0$  obtained from the frequency domain analysis are listed in Table I for the three measurements shown in Fig. 3(a). The excellent agreement between the  $f_c$  and  $S_0$  values obtained from the time domain and the frequency domain data further confirms that the Lorentzian noise observed in the frequency domain results from the RTS current fluctuations in the time domain.

The RTS amplitude  $\Delta I$  as a function of the forward current  $I$  is plotted in the inset of Fig. 3(a). As can be seen from the dashed line fit in the figure,  $\Delta I$  is linearly proportional to  $I$ . This agrees with the theoretically predicted linear dependence of the RTS amplitude on current based on carrier trapping at junction interfaces.<sup>17</sup>

Finally, the semi-log plot of  $\tau_{up}/\tau_{down}$  as a function of forward bias voltage for Measurement 1 is shown in Fig. 3(c). The extracted  $\tau_{up}$  and  $\tau_{down}$  values are 3.50 and 2.81 ms, 5.81 and 8.55 ms, 3.04 and 6.29 ms, and 0.71 and 3.17 ms at a forward bias of 1.04, 1.97, 2.41, and 2.73 V, respectively. Assuming RTS noise is caused by trapping and detrapping of carriers at defects, the ratio of  $\tau_{up}$  to  $\tau_{down}$  can be calculated using the grand partition function as<sup>18</sup>

TABLE I. The values of  $\tau_{up}$ ,  $\tau_{down}$ ,  $f_c$ , and  $S_0$  obtained from the time domain analysis and the values of  $f_c$  and  $S_0$  obtained from the frequency domain analysis for Measurements 1, 2, and 3 shown in Fig. 3(a). The time domain  $f_c$  and  $S_0$  values are calculated from  $\tau_{up}$ ,  $\tau_{down}$ , and  $\Delta I$  values obtained from the measured RTS current fluctuations using Eq. (2). The frequency domain values are extracted by a Lorentzian fitting of the data in Fig. 3(a), similar to that shown in Fig. 2(b).

Measurement	$\tau_{up}$ (ms)	$\tau_{down}$ (ms)	$f_c$ (time domain) (Hz)	$f_c$ (frequency domain) (Hz)	$S_0$ (time domain) ( $A^2/Hz$ )	$S_0$ (frequency domain) ( $A^2/Hz$ )
1	5.81	8.55	46	40	$1.9 \times 10^{-17}$	$2.1 \times 10^{-17}$
2	4.35	2.58	98	125	$6.2 \times 10^{-18}$	$4.0 \times 10^{-18}$
3	0.18	0.13	2144	2525	$3.6 \times 10^{-19}$	$4.0 \times 10^{-19}$

$$\frac{\tau_{up}}{\tau_{down}} = \frac{f_T}{1 - f_T} = \frac{1}{g} \cdot \exp\left(\frac{E_F - E_T}{kT}\right), \quad (3)$$

where  $f_T$  is the probability that the trap level is occupied by an electron,  $g$  is the trap degeneracy factor (assumed to be 1),  $E_F$  is the Fermi level, and  $E_T$  is the trap level. From Fig. 3(c) and Eq. (3), we can extract the zero-bias trap level with respect to the Fermi level as  $E_F - E_T = 32.7$  meV.

In conclusion, we have experimentally characterized the noise properties of CNT film-Silicon Schottky junctions under forward bias, which shows the superposition of a  $1/f$  and a Lorentzian noise component. The  $1/f$  noise component is stable and has the dependence  $S_I \propto I$ , while the Lorentzian noise is temporally unstable. Asymmetric two-level RTS fluctuations in the time domain were also observed and simultaneously recorded. Time durations of the up and down states are found to follow a Poisson distribution, as theoretically expected. The characteristic frequency and the plateau value extracted from the Lorentzian noise component show good agreement with the values calculated from the average lifetime of the up and down states, and the RTS amplitude extracted from the time-domain measurements. This confirms that the Lorentzian noise spectrum results from the RTS current fluctuations in the time domain. The origin of the RTS noise is most likely interface traps at the CNT film-Si junction causing fluctuations in the Schottky barrier height. The zero-bias trap level is extracted to be 32.7 meV below the Fermi level. Another possible origin of the RTS noise could be the presence of a thin native oxide layer at the CNT film-Si interface. Further work is needed to identify the microscopic origins of the RTS noise in detail. These results provide fundamental insights into the noise properties of CNT film-silicon junctions and are important for applications of CNT films as transparent and conductive electrodes in silicon-based photonic and photovoltaic devices, as well as sensors.

This work was funded by the UF Research Opportunity Fund. The authors thank Professor A. G. Rinzler and

Dr. Z. Wu for providing CNT films and Dr. A. Behnam and J. L. Johnson for help with microfabrication.

- <sup>1</sup>J. van de Lagemaat, T. M. Barnes, G. Rumbles, S. E. Shaheen, T. J. Coutts, C. Weeks, I. Levitsky, J. Peltola, and P. Glatkowski, *Appl. Phys. Lett.* **88**, 233503 (2006).
- <sup>2</sup>J. Li, L. Hu, L. Wang, Y. Zhou, G. Grüner, and T. J. Marks, *Nano Lett.* **6**, 2472 (2006).
- <sup>3</sup>A. Behnam, J. L. Johnson, Y. Choi, M. G. Ertosun, A. K. Okyay, P. Kapur, K. C. Saraswat, and A. Ural, *Appl. Phys. Lett.* **92**, 243116 (2008).
- <sup>4</sup>Z. Li, V. P. Kunets, V. Saini, Y. Xu, E. Dervishi, G. J. Salamo, A. R. Biris, and A. S. Biris, *ACS Nano* **3**, 1407 (2009).
- <sup>5</sup>A. D. Pasquier, H. E. Unalan, A. Kanwal, S. Miller, and M. Chhowalla, *Appl. Phys. Lett.* **87**, 203511 (2005).
- <sup>6</sup>Z. Wu, Z. Chen, X. Du, J. M. Logan, J. Sippel, M. Nikolou, K. Kamaras, J. R. Reynolds, D. B. Tanner, A. F. Hebard, and A. G. Rinzler, *Science* **305**, 1273 (2004).
- <sup>7</sup>A. Behnam, N. A. Radhakrishna, Z. Wu, and A. Ural, *Appl. Phys. Lett.* **97**, 233105 (2010).
- <sup>8</sup>S. D. Gobbo, P. Castrucci, M. Scarselli, L. Camilli, M. D. Crescenzi, L. Mariucci, A. Valletta, A. Minotti, and G. Fortunato, *Appl. Phys. Lett.* **98**, 183113 (2011).
- <sup>9</sup>Y. Jia, J. Wei, K. Wang, A. Cao, Q. Shu, X. Gui, Y. Zhu, D. Zhuang, G. Zhang, B. Ma, L. Wang, W. Liu, Z. Wang, J. Luo, and D. Wu, *Adv. Mater.* **20**, 4594 (2008).
- <sup>10</sup>P. Wadhwa, B. Liu, M. A. McCarthy, Z. Wu, and A. G. Rinzler, *Nano Lett.* **10**, 5001 (2010).
- <sup>11</sup>F. Liu, K. L. Wang, D. Zhang, and C. Zhou, *Appl. Phys. Lett.* **89**, 243101 (2006).
- <sup>12</sup>P. G. Collins, M. S. Fuhrer, and A. Zettl, *Appl. Phys. Lett.* **76**, 894 (2000).
- <sup>13</sup>E. S. Snow, J. P. Novak, M. D. Lay, and F. K. Perkins, *Appl. Phys. Lett.* **85**, 4172 (2004).
- <sup>14</sup>A. Behnam, A. Biswas, G. Bosman, and A. Ural, *Phys. Rev. B* **81**, 125407 (2010).
- <sup>15</sup>A. Behnam, Y. Choi, L. Noriega, Z. Wu, I. Kravchenko, A. G. Rinzler, and A. Ural, *J. Vac. Sci. Technol. B* **25**, 348 (2007).
- <sup>16</sup>M. Y. Luo, G. Bosman, A. Van Der Ziel, and L. L. Hench, *IEEE Trans. Electron Devices* **35**, 1351 (1988).
- <sup>17</sup>M. von Haartman, M. Sanden, M. Ostling, and G. Bosman, *J. Appl. Phys.* **92**, 4414 (2002).
- <sup>18</sup>M. J. Kirton, M. J. Uren, S. Collins, M. Schulz, A. Karmann, and K. Scheffer, *Semicond. Sci. Technol.* **4**, 1116 (1989).
- <sup>19</sup>H. Rao and G. Bosman, *J. Appl. Phys.* **106**, 103712 (2009).
- <sup>20</sup>G. Ghibaudo and T. Boutchacha, *Microelectron. Reliab.* **42**, 573 (2002).
- <sup>21</sup>S. Machlup, *J. Appl. Phys.* **25**, 341 (1954).